

1

2 **Supplementary Information for**

3 **The limitations of extending nature's color palette in correlated, disordered systems**

4 **Gianni Jacucci, Silvia Vignolini and Lukas Schertel**

5 **Silvia Vignolini**

6 **E-mail: sv319@cam.ac.uk**

7 **This PDF file includes:**

8 Supplementary text

9 Figs. S1 to S3

10 Table S1

11 SI References

12 Supporting Information Text

13 1. Role of form factor and structure factor in direct photonic glasses

14 The optical appearance of a material depends on the illumination source, the observer's receptors sensitivity spectrum and the
15 reflection properties of the material. The latter is characterized by the reflection spectrum $R(\lambda)$. In the limit of non-absorbing,
16 diffusive media it can be calculated via the transmittance of a slab shaped sample which is directly related to the optical
17 density ℓ^*/L , with ℓ^* the transport mean free path and L the sample thickness (1). ℓ^* defines the length scale after which
18 isotropy in the multiple scattering is reached and is inversely related to the turbidity of a multiple scattering sample.

19 For high density PG made of monodisperse spheres with radius r and filling fraction ff a recently developed scattering
20 model can be used to calculate the scattering strength λ/ℓ^* (with λ the wavelength of the incident light) from the anisotropy
21 factor $\langle \cos \theta \rangle$ and scattering cross section (2) σ_s :

$$22 \quad \frac{\lambda}{\ell^*} = \frac{\lambda(1 - \langle \cos \theta \rangle)3ff\sigma_s}{4\pi r^3} \quad [1]$$

23 Expressing σ_s via the angular integral over the local scattering intensity $I(\theta) = F(\theta)S(\theta)$

$$24 \quad \frac{\lambda}{\ell^*} = \frac{(1 - \langle \cos \theta \rangle)3ff}{16\pi^2} \left(\frac{\lambda}{r}\right)^3 \int_0^\pi F(\theta)S(\theta) \sin \theta d\theta, \quad [2]$$

25 shows that this calculation allows to disentangle the scattering contributions of the Mie form-factor $F(\theta)$ (3) and the structure-
26 factor $S(\theta)$ (4). Note that in this formulation both $\langle \cos \theta \rangle$ and σ_s depend strongly on the choice of an effective refractive
27 index of the material n_{eff} (2, 5). In this work, the energy coherent potential approximation (ECPA) refractive index is used as
28 it accounts for near field coupling of the scatterers. (6) In summary, the reflection spectrum $R(\lambda)$ of a PG material can be
29 calculated via ℓ^* and depends on λ , r , ff , the scatterer refractive index n and the refractive index of the surrounding medium
30 n_m .

31 In Figure S1, we use this model to calculate the scattering strength for various refractive index contrasts: weakly scattering
32 (e.g. index matched PG, $n = 1.3$, blue solid line), polymer-like systems ($n = 1.5$, green solid line) and highly scattering (e.g.
33 titanium dioxide PG, $n = 2.5$, red solid line). We observe that the contribution from structural correlation (black dashed line)
34 remains constant for all refractive indices while the contribution from Mie scattering (colored dashed lines) strongly scales with
35 refractive index contrast. For high refractive index contrast ($n = 2.6$) the scattering strength is dominated by the contribution
36 from the form-factor, while in an intermediate regime ($n = 1.5$) the position and amplitude of the scattering resonances is
37 equally influenced by the structural correlation and the form-factor contribution, especially for the first multiple Mie-scattering
38 resonance. For low refractive index contrast ($n = 1.3$) the main spectral feature is strongly correlated with the position of the
39 structural correlation.

40 2. Role of refractive index on the optical response of inverse photonic glasses

41 Figure S2, generalizing what reported in Figure 2 of the main text, shows the importance of the refractive index on the optical
42 response of inverse PGs. Indeed, as discussed in the main text, the structural color of PGs is the result of the balance of
43 single-particle and structural contributions. The spectral response of inverse PGs with $n=2.60$ is dominated by single-particle
44 scattering; while for $n=1.30$ the structure factor contribution prevails.

45 3. Role of different ensemble parameters on the optical response of inverse photonic glasses

46 Figure S3 shows how the optical response of PGs is effected by various ensemble parameters. As discussed in further details in
47 the main text, inverse PGs are more robust than direct PGs to changes of the polydispersity (Figure S3b). Moreover, when
48 increasing the thickness the presence of multiple scattering leads to an increase of the incoherent background - therefore
49 decreasing the purity and saturation of the optical response (Figure S3a). Finally, decreasing the filling fraction of air inclusions
50 leads to a red-shifted peak which is less pronounced than its counterpart at $ff=0.5$ (Figure S3c).

Table S1. Chromaticity values displayed in Figure 4a

PGs structure	<i>x</i> value	<i>y</i> value	displayed spectrum
direct	0.321	0.324	Fig SI.3 in ref. (7)
inverse	0.363	0.314	Fig 2b
poly	0.375	0.346	Fig S3c
low Δn	0.375	0.256	Fig 3a
coated	0.37	0.362	Fig 3b
combined	0.508	0.398	Fig 3c
RGB	0.64	0.33	-

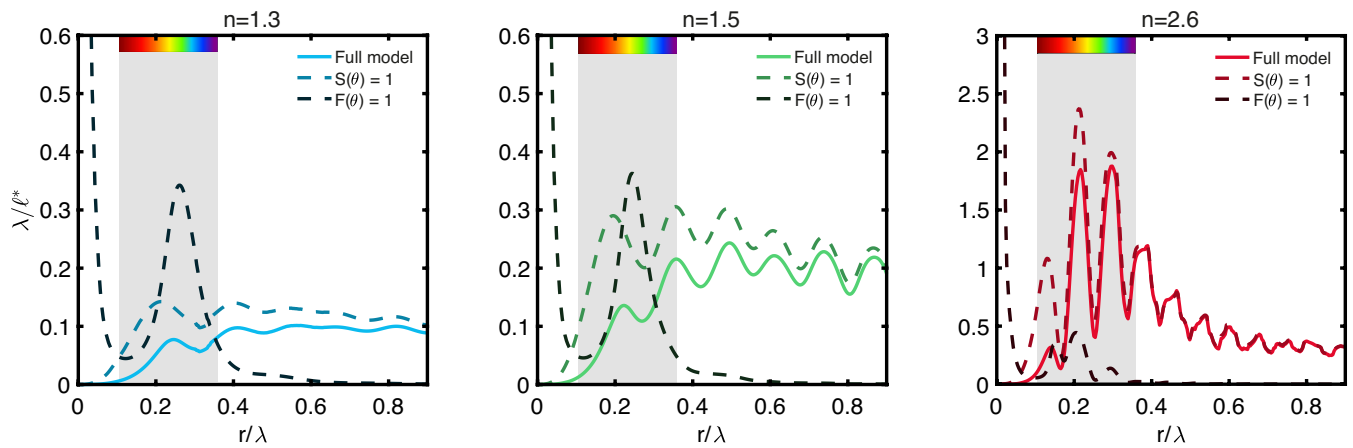


Fig. S1. ECPA scattering model: scattering strength λ/ℓ^* with varying size ratio r/λ calculated from Equation 2, for Mie-resonance contributions only ($S(\theta) = 1$) and for structural contributions only ($F(\theta) = 1$) for three refractive indices of the scattering particles $n = 1.3$, $n = 1.6$ and $n = 2.6$. For the surrounding medium a refractive index of $n_m = 1.0$ was assumed. The visible wavelength range indicated by the grey shaded area refers to particles with $r=130\text{nm}$. Models taking into account only structural contributions are scaled by a factor 0.01.

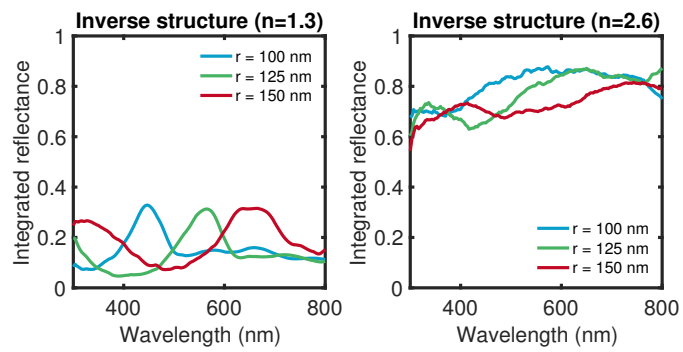


Fig. S2. Simulated optical response for inverse photonic glasses with refractive index of $n=1.3$ and $n=2.6$, left and right panel, respectively. All the simulated structures have a thickness of $3 \mu m$, $ff = 0.5$.

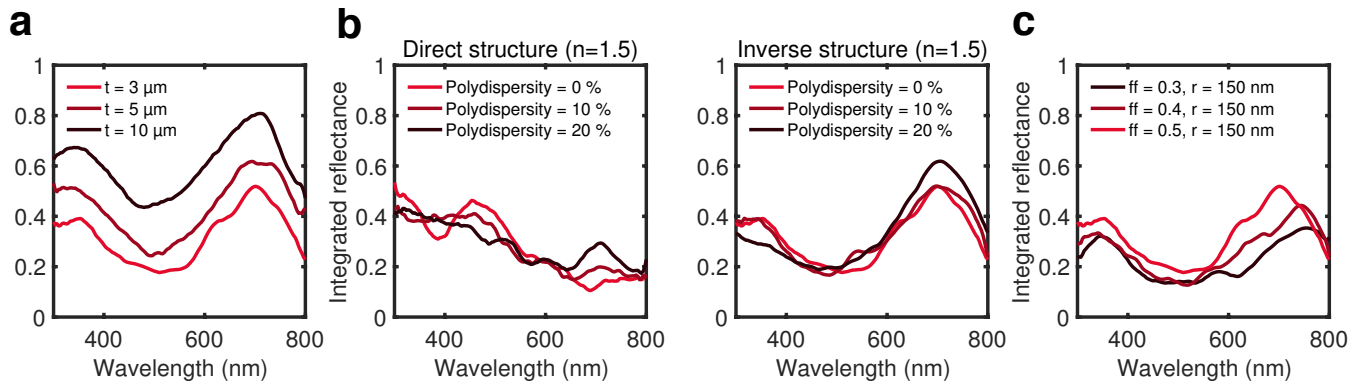


Fig. S3. a) Effect of the thickness on the optical response of inverse photonic glasses; an increase in the thickness leads to a broadband increase of the reflectance, decreasing the colour purity. b) Simulated optical response for direct and inverse photonic glasses in function of particles' polydispersity. The spectral peak is more resistant to polydispersity in the case of inverse PGs, where it is mainly originating from structural contributions. c) Effect of the filling fraction on the optical response of inverse photonic glasses; a decrease in the filling fraction leads to a red-shifted peak, due to an increase of the effective refractive index of the system, with lower intensity. All the simulated structures have an average size of the scatterers of $r = 150 \text{ nm}$ and, when not mentioned differently in the caption, a thickness of $3 \mu\text{m}$, $ff = 0.5$ and $n=1.50$.

51 **References**

- 52 1. N Garcia, AZ Genack, AA Lisyansky, Measurement of the transport mean free path of diffusing photons. *Phys. Rev. B* **46**,
53 14475–14479 (1992).
- 54 2. GJ Aubry, et al., Resonant transport and near-field effects in photonic glasses. *Phys. Rev. A* **96**, 043871 (2017).
- 55 3. CF Bohren, DR Huffman, *Absorption and Scattering of Light by Small Particles*. (Wiley, New York), (1998).
- 56 4. JK Percus, GJ Yevick, Analysis of classical statistical mechanics by means of collective coordinates. *Phys. Rev.* **110**, 1–13
57 (1958).
- 58 5. L Schertel, et al., Tunable high-index photonic glasses. *Phys. Rev. Mater.* **3**, 015203 (2019).
- 59 6. K Busch, CM Soukoulis, Transport properties of random media: A new effective medium theory. *Phys. Rev. Lett.* **75**,
60 3442–3445 (1995).
- 61 7. L Schertel, et al., The structural colors of photonic glasses. *Adv. Opt. Mater.* **7**, 1900442 (2019).